Homogenization approach to the behavior of suspensions of noncolloidal particles in yield stress fluids

Xavier Chateau*, Guillaume Ovarlez, Kien Luu Trung
Laboratoire des Matériaux et des Structures du Génie Civil
Institut Navier (UMR113 LCPC-ENPC-CNRS)
2 Allée Kepler, 77420 Champs sur Marne, France.

Synopsis

The behavior of suspensions of rigid particles in a non-Newtonian fluid is studied in the framework of a nonlinear homogenization method. Estimates for the overall properties of the composite material are obtained. In the case of a Herschel-Bulkley suspending fluid, it is shown that the properties of a suspension with overall isotropy can be satisfactory modeled as that of a Herschel-Bulkley fluid with an exponent equal to that of the suspending fluid. Estimates for the yield stress and the consistency at large strain rate levels are proposed. These estimates compare well to both experimental data obtained by Mahaut et al. (2007) and to experimental data found in the literature.

I Introduction

Heterogeneous systems consisting of particles suspended in a fluid medium make up in a wide variety of materials of practical interest, both natural (slurries, debris flows, lavas, ...) or man-made (concretes, food pastes, paints, cosmetics, ...). This abundance explains why the behavior of these materials have been extensively studied from both a theoretical and an experimental point of view.

In the framework of man-made materials, it does not seem to exist a well established method to obtain a material with given rheological characteristics from components having known properties despite the fact that is is a problem encountered in numerous industrial processes. The set-up of such a methodology requires the ability to predict the overall behavior of the material from that of its constituents. A general answer for this problem has yet to be found.

The main difficulty in modeling the behavior of suspensions comes from the fact that the material is multiscale and contains many interacting constituents. Experimental data show that the overall rheological properties of a suspension depend upon the shape and size of the particles, the interaction between particles (colloidal or noncolloidal), the interaction between the particles and the suspending fluid (hydrodynamic), the properties of the suspending fluid (Newtonian or not) and the type of flow the suspension is subjected to.

In this paper, we focus on suspensions made up of noncolloidal particles dispersed in a yield stress fluid such as suspensions made up of a coarse fraction and a colloidal fraction. If the colloidal particles are much smaller than the coarse ones, the latter interact with the other components of the suspension only through hydrodynamic interactions: they see a homogeneous phase fluid which behavior is that of the colloidal suspension [Sengun and Probstein (1989a,b); Ancey and Jorrot (2001)].

Like for any other suspensions, the rheological properties of non-Newtonian suspensions depend upon the shape, the surface texture and the size distribution of the coarse particles.

*corresponding author: xavier.chateau@lcpc.fr

In addition to experimental approaches, modeling the behavior of non-Newtonian suspensions using their constituents characteristics in the framework of numerical methods appears promising because of the ability of these methods to track the particles localization in the suspension and to account for several interparticle interactions. Solving the problem for noncolloidal particles immersed in a Newtonian fluid is feasible using modern computers and provides useful results [Brady (2001)]. The most serious drawback of these methods to their generalization to non-Newtonian suspending fluid is the fact that the Newtonian hydrodynamic force applied to the particle is evaluated by means of close form equations depending on the macroscopic strain rate and on the particle velocity relative to the bulk fluid [Bossis and Brady (1984); Brady and Bossis (1988)]. Thanks to these relations, it is not necessary to solve the continuous Stokes equation in the bulk fluid in order to simulate the behavior of the suspension. This enables to simulate the flow of representative elementary volume of a suspension containing numerous particles at a reasonable computational cost. To our knowledge, such an equation does not exist for particles immersed in a yield stress fluid, which prevents a generalization of the method to be easily proposed.

Trying to evaluate the velocity field in the bulk yield stress fluid by means of a finite element method is such a time consuming task that no situation of practical interest can be solved using these tools today [Johnson and Tezduyar (1997); Roquet and Saramito (2003); Yu and Wachs (2007)].

To obtain estimates for the overall characteristics of non-Newtonian suspensions, the change of scale method appears then to be a powerful tool. As a reminder homogenization technique aims at identifying the macroscopic properties of a material modeled as a continuous medium from those of their constituents. The first results in this field were obtained by Einstein (1906) for the viscosity of a dilute suspension. Since, different problems have been studied such as the viscosity of multimodal suspensions [Farris (1968)], the viscosity of concentrated suspensions [Krieger and Dougherty (1959); Frankel and Acrivos (1967)], the effect of the shape and orientation of particles on the behavior of Newtonian suspensions [Batchelor (1971)], the effect of interparticle interactions [Batchelor and Green (1972)] or the effect of Brownian motions on the overall behavior [Batchelor (1977); Russel et al. (1995)].

It is worth noticing that it has not been possible to obtain exact solutions for most of the problems cited above; generally, only estimates of the overall characteristics of the suspension have been obtained. This situation is very similar to the one prevailing in the field of homogenization approaches to the behavior of solid materials [Zaoui (2002)]. This is not surprising since the two problems are very similar as it has been recognized by Batchelor and Green (1972). The main difference comes from the fact that the morphology of the heterogeneities within the representative elementary volume is a given for solid materials whereas it is an unknown for particle suspensions since the flow of the representative elementary volume of suspension and the morphology of the particles are coupled

Interestingly, novel developments have taken place in nonlinear continuum micromechanics in the last twenty years so that both estimates and variational bounds are now available [see Suquet (1998) for a review]. Because of the similarities between the solid problem with the liquid one, it is quite natural to address the modeling of the behavior of non-Newtonian suspensions within this framework.

The aim of this paper is to provide a first approach to the overall behavior of a suspension of non-Brownian and noncolloidal particles immersed in an incompressible yield stress fluid. First, the main features of the homogenization approach to the behavior of non-Newtonian suspensions are recalled. Then, the secant-method of Castañeda (1991) and Suquet (1993) is applied in order to estimate the overall behavior of the suspension. The estimates are compared to new experimental results obtained by Mahaut et al. (2007) and to experimental results of the literature in the next part. Finally, the validity of the theoretical approach is discussed before some general conclusions are drawn.

II Homogenized behavior

We examine the overall behavior of a suspension, the liquid phase of which is homogeneous and nonlinear. We restrict ourselves to the situation where the constitutive behavior of the fluid is characterized by an energy function $w(\boldsymbol{d})$ where $\tilde{d} = \sqrt{2\boldsymbol{d} : \boldsymbol{d}}$ denotes the second invariant of the Eulerian strain rate tensor $\boldsymbol{d}$. The Cauchy stress $\boldsymbol{\sigma}$ is obtained by differentiation of the potential w with respect to the strain rate tensor $\boldsymbol{d}$ if w is differentiable. Otherwise, the derivative should be interpreted as the subdifferential of convex analysis.

The condition of naught strain for the particles can also be written in term of a dissipation potential with w defined by

$$w(\boldsymbol{d}) = 0 \text{ if } \boldsymbol{d} = 0 \quad w(\boldsymbol{d}) = \infty \text{ if } \boldsymbol{d} \neq 0 \tag{1}$$

Thus, the suspension is made of a heterogeneous medium, the behavior of which is described by

$$\boldsymbol{\sigma} = \frac{\partial w}{\partial \boldsymbol{d}}(\boldsymbol{d}, \underline{x}) \tag{2}$$

w being a strict convex function. The location in the representative elementary volume is defined by the position vector $\underline{x}$.

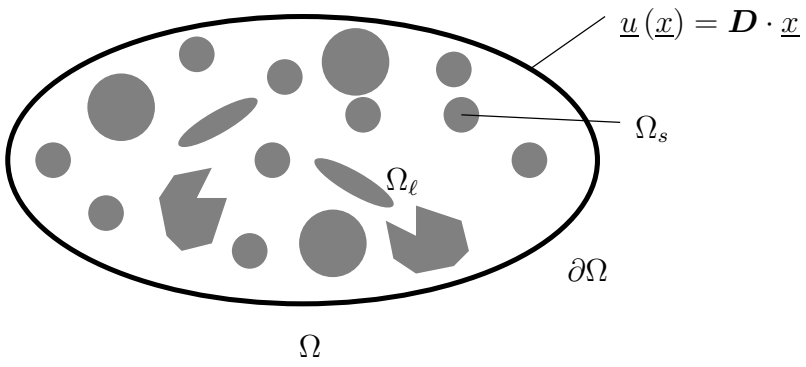

Figure 1: The representative elementary volume of the suspension submitted to a macroscopic strain rate loading (Hashin boundary condition).

It is assumed that it is possible to define a representative elementary volume of the suspension occupying a domain Ω with boundary $\partial\Omega$ such that it is large enough to be of typical composition and its overall properties do not depend on the way it is loaded at the macroscopic scale. Ω_s and Ω_ℓ denote the solid and the liquid domain respectively. The volume fraction of particles φ is the ratio of the volume fraction of Ω_s in Ω. For simplicity, it is assumed that the boundary of Ω is located in the liquid domain as depicted in Fig. 1. At the microscopic scale, Ω is considered as a structure. $< a >$ (resp. $< a >_\alpha$ with $\alpha = s, \ell$) denotes the average of a over Ω (resp. Ω_α). The liquid phase is homogeneous. We adopt an Eulerian description of the movement and we restrict our attention to the situations where the evolutions of the system are quasistatics (*i.e.* inertial effects are negligible) and all the long range forces other than the hydrodynamic ones are negligible.

As shown by Hill (1963), the overall behavior of the suspension reads:

$$\boldsymbol{\Sigma} = \frac{\partial W}{\partial \boldsymbol{D}}(\boldsymbol{D}) \quad \text{with } W(\boldsymbol{D}) = \min_{\boldsymbol{d} \in \mathcal{C}(\boldsymbol{D})} \langle w(\boldsymbol{d}) \rangle \tag{3}$$

where $\mathcal{C}(\boldsymbol{D})$ denotes the set of Eulerian strain rate fields kinematically admissible with $\boldsymbol{D}$. It is recalled that a strain rate field $\boldsymbol{d}$ defined over Ω is said to be kinematically admissible with

$\boldsymbol{D}$ if exists a velocity field $\underline{u}$ defined over Ω, complying with the Hashin condition

$$(\forall\, \underline{x} \in \partial\Omega) \quad \underline{u}\,(\underline{x}) = \boldsymbol{D} \cdot \underline{x} \tag{4}$$

such as:

$$(\forall\, \underline{x} \in \Omega) \qquad \boldsymbol{d}\,(\underline{x}) = \frac{1}{2}\left(\mathbf{grad}\,\underline{u}\,(\underline{x}) + {}^{\mathrm{t}}\mathbf{grad}\,\underline{u}\,(\underline{x})\right) \tag{5}$$

When the fluid obeys a Herschel-Bulkley law with a yield stress τ_c, a consistency η and a power law exponent $n > 0$, the dissipation potential reads:

$$\begin{aligned} w\,(\boldsymbol{d}) &= \tau_c\,\tilde{d} + \frac{\eta}{n+1}\tilde{d}^{n+1} \quad \text{if} \quad \mathrm{tr}\boldsymbol{d} = 0 \\ w\,(\boldsymbol{d}) &= \infty \qquad\qquad\qquad\quad \text{if} \quad \mathrm{tr}\boldsymbol{d} \neq 0 \end{aligned} \tag{6}$$

Then the fluid's state equation reads

$$\begin{aligned} \boldsymbol{d} &= 0 \qquad\qquad\qquad\qquad\quad \text{if} \quad \sqrt{\boldsymbol{s} : \boldsymbol{s}/2} < \tau_c \\ \boldsymbol{s} &= \left(\tau_c + \eta\tilde{d}^n\right)\frac{\boldsymbol{d}}{\tilde{d}} \quad \mathrm{tr}\boldsymbol{d} = 0 \qquad \text{if} \quad \sqrt{\boldsymbol{s} : \boldsymbol{s}/2} \geq \tau_c \end{aligned} \tag{7}$$

where $p = -\mathrm{tr}\boldsymbol{\sigma}/3$ is the hydrostatic pressure, $\boldsymbol{s} = \boldsymbol{\sigma} + p\boldsymbol{\delta}$ the deviator of $\boldsymbol{\sigma}$ and $\boldsymbol{\delta}$ the second order unit tensor. As it is common for incompressible materials, the pressure p is not determined by the state law. Considering that the particles are rigid and that the bearing fluid is homogeneous and incompressible, it is easily shown from Eq. (3) that the macroscopic potential is also defined by

$$W\,(\boldsymbol{D}) = \min_{\boldsymbol{d} \in \mathcal{G}(\boldsymbol{D})} (1-\varphi)\left[\tau_c \left\langle \tilde{d} \right\rangle_\ell + \frac{\eta}{n+1}\left\langle \tilde{d}^{n+1} \right\rangle_\ell\right] \qquad \text{if } \mathrm{tr}\boldsymbol{D} = 0 \tag{8}$$

where $\mathcal{G}\,(\boldsymbol{D})$ denotes the subset of $\mathcal{C}\,(\boldsymbol{D})$ which elements comply with the naught strain rate constraint over the domain occupied by the particles and the incompressible constraint over the fluid domain. Of course, the set $\mathcal{G}\,(\boldsymbol{D})$ is only defined for macroscopic strain rate complying with the condition $\mathrm{tr}\boldsymbol{D} = 0$. Eq. (8) is completed by the condition $W\,(\boldsymbol{D}) = \infty$ if $\mathrm{tr}\boldsymbol{D} \neq 0$, which enforced the incompressible constraint at the macroscopic level.

The set $\mathcal{G}\,(\boldsymbol{D})$ being convex, the minimization problem (8) admits only one solution, which ensures the validity of the method. The identification of the macroscopic behavior of the suspension from Eq. (3) or Eq. (8) requires the resolution of a continuous convex minimization problem. This problem of minimization has to be solved for each morphology of the suspension defined by the shape of the particles and the distribution of the particles within the suspension. Of course, it is not possible to solve this problem in most situations of practical interest.

To remedy this difficulty, various estimation techniques of the macroscopic behavior have been proposed, in particular, by Castañeda (1991, 1996, 2003) and Suquet (1993).

The key feature in these methods is the use of a rigorous variational principle (Eq. 3 for the yield stress fluid suspensions) to determine the best possible choice of a "linear comparison composite" to estimate the effective behavior of the nonlinear one. A detailed description of these methods is beyond the scope of the present paper. The reader is referred to [Suquet (1998)] for a more detailed review.

In the following, we obtained estimates relevant to our problem in the framework of a simple approach which does make use explicitly of the variational Eq. 3. The main features of the method used to obtain these estimates are recalled in the following section (largely inspired by the presentation of Suquet (1997)) for completeness of the paper.

III Secant estimate of the behavior

It is assumed that the solid particles are isotropically distributed over the representative elementary volume. The macroscopic behavior of the suspension is therefore also isotropic.

It is possible to write the behavior of the nonlinear fluid in the following form

$$\boldsymbol{\sigma} = 2\mu^{\mathrm{sct}}(\tilde{d})\boldsymbol{d} - p\boldsymbol{\delta} \tag{9}$$

where $\mu^{\mathrm{sct}}(\tilde{d})$ denotes the secant modulus of the fluid phase. The secant modulus is no more than the apparent viscosity of the fluid, as depicted in Fig. 2.

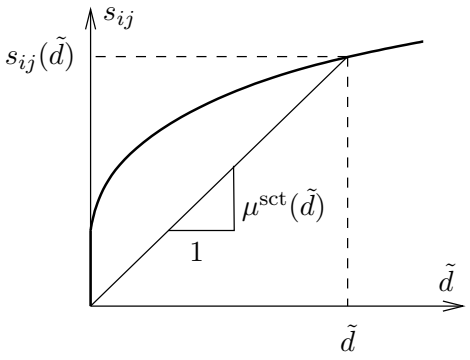

Figure 2: Secant modulus formulation of nonlinear incompressible isotropic fluid.

Using Eq. (9) for the state equation of the suspending fluid, it is possible to replace the original nonlinear problem of homogenization by a linear homogenization problem for a suspension of rigid particles immersed in a heterogeneous incompressible isotropic fluid with apparent viscosity $\eta\left(\underline{x}\right) = \mu^{\mathrm{sct}}\left(\underline{x}, \tilde{d}\left(\underline{x}\right)\right)$.

Then, the difficulty which remains to be solved is to calculate, or to estimate, the field $\tilde{d}$ over the domain occupied by the fluid phase in the representative elementary volume. Since it is impossible to analytically determine the local response of the nonlinear fluid, it is impossible to compute the secant modulus field over the representative elementary volume. Then an approximation has to be introduced to make analytic calculations feasible. The approximation for secant methods consists of replacing the secant modulus field over the representative elementary volume by a modulus which is uniform over subdomains of the representative elementary volume. In this paper, we consider only one domain for the liquid phase to simplify. Then the secant modulus is uniform over the fluid phase. This estimate reads:

$$(\forall\ \underline{x} \in \Omega_\ell) \quad \mu^{\mathrm{sct}}\left(\underline{x}, \tilde{d}\left(\underline{x}\right)\right) \simeq \mu_\ell^{\mathrm{sct}}(\tilde{d}_\ell^{\mathrm{eff}}) \tag{10}$$

where $\tilde{d}_\ell^{\mathrm{eff}}$ is an equivalent effective strain rate which remains to be defined as a function of the mean value of the field $\tilde{d}$ in the fluid phase, and thus, of the value of the macroscopic strain rate. The replacement of the field of heterogeneous secant modulus defined over the fluid phase by a homogeneous field simplifies considerably the resolution of the problem. Consequently, the estimate technique of the nonlinear macroscopic behavior includes three steps:

1. First of all, it is necessary to solve a linear homogenization problem for a suspension of particles immersed in an isotropic homogeneous fluid of viscosity μ_ℓ. If the suspension is isotropic at the macroscopic scale, the macroscopic behavior is characterized by a macroscopic viscosity proportional to the viscosity of the fluid, the coefficient of proportionality depending on the morphology of the particles. As this problem has been the subject of

many works, numerous results and estimates are available in the literature dealing with the rheology of suspensions or the homogenization to the behavior of heterogeneous linear materials. Let $g(\varphi)$ denotes the coefficient of proportionality linking the macroscopic viscosity to the microscopic viscosity.

$$\mu^{\text{hom}} = \mu_\ell \, g(\varphi) \tag{11}$$

2. Then, one must choose a measure of the effective strain rate for the fluid phase. As the considered material is isotropic at the microscopic scale, the strain rate is characterized by the second order moment of the quantity $\tilde{d}$ defined by:

$$\tilde{d}_\ell^{\text{eff}} = \sqrt{\langle \tilde{d}^2 \rangle_\ell} \tag{12}$$

This choice corresponds to the modified approach described by Suquet (1997). Castañeda (1991) demonstrated that this choice is optimal in the framework of a variational approach to the solution of the nonlinear homogenization problem under consideration. It would have been simpler to choose $\tilde{d}_\ell^{\text{eff}} = \widetilde{< \boldsymbol{d} >_\ell}$, a quantity easily computed from the egality $\langle \boldsymbol{d} \rangle_\ell = \boldsymbol{D}/(1-\varphi)$. Unfortunately, Suquet (1997) showed that estimates of the overall properties of the heterogeneous material obtained using this effective liquid strain rate are less accurate than those obtained using Eq. (12).

3. Finally, the nonlinear character of the problem is taken into account by integrating into the relation of homogenization (11) linking μ^{hom} to the viscosity of the liquid phase, the fact that the value of the fluid viscosity depends on $\tilde{d}_\ell^{\text{eff}}$. As $\tilde{d}_\ell^{\text{eff}}$ depends on the value of the macroscopic strain rate $\boldsymbol{D}$, the value of the macroscopic secant modulus also depends on the value of $\boldsymbol{D}$. The only difficulty implementing this step is the calculation of $\tilde{d}_\ell^{\text{eff}}$ as a function of $\boldsymbol{D}$ for the particular homogenization scheme used. It has been shown by Kreher (1990) that:

$$\langle \tilde{d}^2 \rangle_\ell = \frac{1}{1-\varphi} \frac{\partial \mu^{\text{hom}}}{\partial \mu_\ell} \tilde{D}^2 = \frac{1}{1-\varphi} g(\varphi) \tilde{D}^2 \tag{13}$$

By remplacing μ_ℓ by μ^{sct} in the relation of linear homogenization Eq. (11) and then by combining the obtained equation with the localization Eq. (13), one obtains the following estimate for the macroscopic secant modulus (i.e. apparent viscosity) of any nonlinear materials with any isotropic microstructure:

$$\mu^{\text{hom}}\left(\varphi, \tilde{D}\right) = g(\varphi) * \mu^{\text{sct}}\left(\tilde{d}\right) \quad \text{with} \quad \tilde{d} = \tilde{D}\sqrt{\frac{g(\varphi)}{1-\varphi}} \tag{14}$$

Using notations of Sengun and Probstein (1989b), the apparent viscosity Eqs. (14) reads

$$\eta(\varphi, \dot{\gamma}) = \eta_{\text{cr}}(\varphi) * \eta_{\text{fr}}(\dot{\gamma}_{\text{eff}}) \quad \text{with} \quad \dot{\gamma}_{\text{eff}} = \dot{\gamma}\sqrt{\frac{\eta_{\text{cr}}(\varphi)}{1-\varphi}} \tag{15}$$

which is much more general than Eqs (2.8), (2.9), (4.1) and (4.2) of Sengun and Probstein (1989b) as they allow to take into account any estimate $g(\varphi)$ (*i.e.* $\eta_{\text{cr}}(\varphi)$) of the relative viscosity of a Newtonian suspension. It is worth noting that Eqs. (14) and (15) are valid for any particles shape and dispersity. Interestingly, even if the estimate $g(\varphi)$ does not rely on a morphological model, Eq. (13) allows to estimate the localization factor associated with the relative viscosity function $g(\varphi)$.

Coming back to the Herschel-Bulkley suspension problem, the secant modulus of the suspending fluid reads:

$$\mu^{\text{sct}}\left(\underline{x}, \tilde{d}\left(\underline{x}\right)\right) = \frac{\tau_c}{\tilde{d}\left(\underline{x}\right)} + \eta\left(\tilde{d}\left(\underline{x}\right)\right)^{n-1} \tag{16}$$

Then, putting Eq. (16) into Eq. (14) yields

$$\mu^{\text{hom}}\left(\varphi, \boldsymbol{D}\right) = \frac{\tau_c^{\text{hom}}}{\tilde{D}} + \eta^{\text{hom}}\tilde{D}^{n-1} \tag{17}$$

with:

$$\tau_c^{\text{hom}} = \tau_c\sqrt{(1-\varphi)g(\varphi)} \tag{18}$$

and:

$$\eta^{\text{hom}} = \eta g(\varphi)\left[\frac{g(\varphi)}{1-\varphi}\right]^{\frac{n-1}{2}} \tag{19}$$

It is therefore predicted that, at the macroscopic scale, the suspension behaves as a Herschel-Bulkley fluid with same exponent as that of the suspending fluid. Overall yield stress and macroscopic consistency are defined by Eqs. (18) and (19). This result does not depend on the scheme (*i.e.* $g(\varphi)$) used to link the viscosity of the bearing fluid to the overall viscosity of the suspension. The quality of the prediction depends thus only on the validity of the assumption that the field $\mu_\ell^{\text{sct}}\left(\underline{x}, \tilde{d}\left(\underline{x}\right)\right)$ can be estimated by the quantity $\mu_\ell^{\text{sct}}(\tilde{d}_\ell^{\text{eff}})$.

IV Experimental validation

An experimental procedure has been designed by Mahaut et al. (2007) which complies with the assumptions made to obtain the theoretical results presented above. As this procedure is described in detail in the paper entitled *Yield stress and elastic modulus of suspensions of noncolloidal particles in yield stress fluids*, no further details concerning the experimental work are given in this paper; we restrict ourselves to comparisons between experimental data and theoretical predictions.

A Elastic modulus vs. yield stress

The accuracy of the estimates obtained in the framework of the theoretical approach presented above for the overall properties of the yield stress suspension depends on the assumption made to take into account the nonlinear behavior of the suspending fluid and on the scheme used to estimate the overall linear behavior of the suspension. It is possible to check experimentally the validity of the assumption made on the heterogeneities of the secant modulus over the liquid domain irrespective of the errors induced by the choice of a particular homogenization scheme. For this, it is enough to remark that Eq. (11) enables to calculate the macroscopic elastic modulus G^{hom} of an isotropic suspension of particles dispersed in an isotropic incompressible linear elastic matrix whose shear modulus is equal to G (both problems pose exactly in the same way provided that $\boldsymbol{d}$ and μ_ℓ be identified with the infinitesimal strain tensor and the elastic shear modulus). As a consequence, it is possible to obtain a general relationship between the dimensionless elastic modulus and the dimensionless yield stress of a suspension of rigid particles dispersed in a yield stress fluid that is true whatever the scheme as long as the particle distribution is isotropic and using an uniform secant modulus estimate is relevant. Combining Eqs. (11),(18) and (19) yields the relations:

$$\tau_c^{\text{hom}}/\tau_c = \sqrt{(1-\varphi)G^{\text{hom}}/G} \tag{20}$$

and

$$\eta^{\text{hom}}/\eta = \sqrt{\frac{\left(G^{\text{hom}}/G\right)^{n+1}}{(1-\varphi)^{n-1}}} \tag{21}$$

Moreover, the yield stress and the consistency not being independent of one another, it is also possible to determine the consistency from the yield stress and the concentration:

$$\eta^{\mathrm{hom}}/\eta = \frac{\left(\tau_c^{\mathrm{hom}}/\tau_c\right)^{n+1}}{(1-\varphi)^n} \tag{22}$$

In Fig. 3, we have plotted the dimensionless yield stress τ_c/τ_c as a function of the dimensionless quantity $\sqrt{(1-\varphi)G^{\mathrm{hom}}/G}$ for all the systems studied by Mahaut et al. (2007). It is recalled that yield stress fluids have a solid linear viscoelastic behavior below the yield stress, so that the macroscopic elastic modulus of the suspensions could be experimentally measured through oscillatory shear measurements. A good agreement between the experimental results

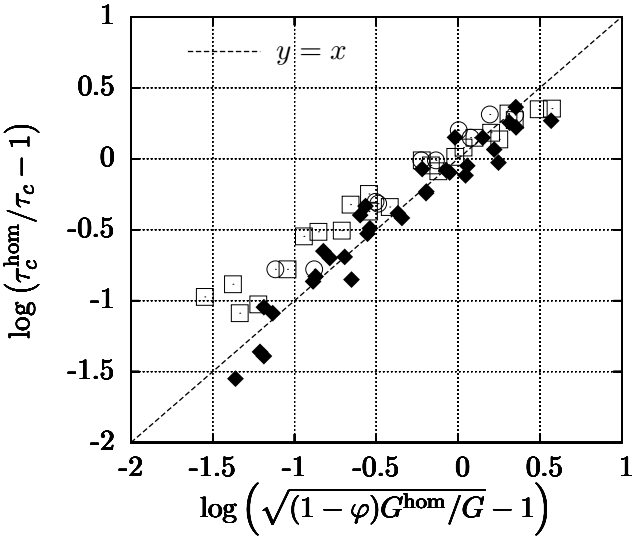

Figure 3: Dimensionless yield stress $\tau_c^{\mathrm{hom}}/\tau_c$ as a function of $\sqrt{(1-\varphi)G^{\mathrm{hom}}/G}$ for all the systems studied by Mahaut et al. (2007). The open square symbols are suspensions of polystyrene and glass beads in bentonite, the open circle symbols are suspensions of glass beads in carbopol while the solid diamond symbols are suspensions of polystyrene and glass beads in emulsion. The figure's coordinates were chosen so that the $y = x$ line represents the theoretical relation (20).

and the micromechanical estimation (20) (which is plotted as a straight line $y = x$ in these coordinates) is observed. These results show that the data are consistent with the assumption that an uniform estimate of the secant modulus over the fluid domain allows to accurately estimate the overall properties of the suspension in the studied situations.

B Elastic modulus

In this section, we summarize the results of the elastic modulus measurements performed on all the materials.

The evolution of the dimensionless modulus G^{hom}/G as a function of the volume fraction φ of noncolloidal particles for all the studied materials are summarized in Fig. 4. It is observed that the experimental data are very well fitted to the Krieger-Dougherty law (Krieger and Dougherty (1959)):

$$\frac{G^{\mathrm{hom}}}{G} = g(\varphi) = \left(1 - \frac{\varphi}{\varphi_m}\right)^{-2.5\varphi_m} \tag{23}$$

The value of the maximum packing fraction $\varphi_m = 0.57$ was fixed by means of a least squares method. This value is very close to the value $\varphi_m = 0.605$ measured locally very recently in dense suspensions of noncolloidal particles in Newtonian fluids by Ovarlez et al. (2006) through

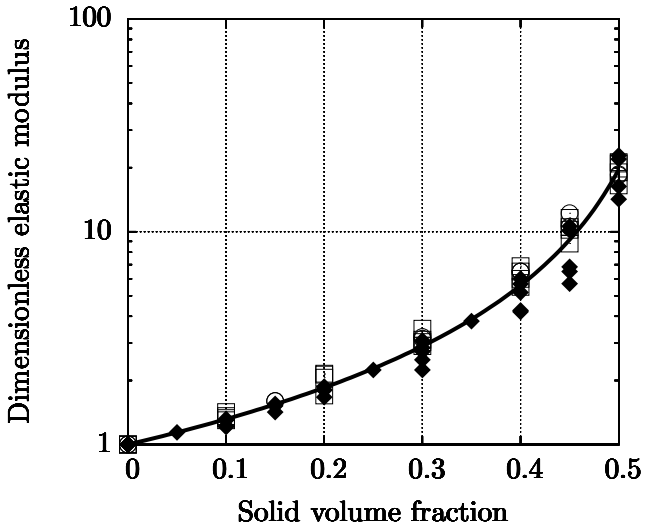

Figure 4: Dimensionless elastic modulus G^{hom}/G vs the beads volume fraction φ for all the systems studied by Mahaut et al. (2007). The open square symbols are suspensions of polystyrene and glass beads in bentonite, the open circle symbols are suspensions of glass beads in carbopol while the solid diamond symbols are suspensions of polystyrene and glass beads in emulsion. The solid line is the Krieger-Dougherty Eq. (23) with $\varphi_m = 0.57$.

MRI techniques. The small discrepancy between the two values of φ_m comes certainly from the anisotropy induced by the flow in the experiments of Ovarlez et al. (2006) as it was also observed in the experiments performed by Parsi and Gadala-Maria (1987).

C Yield stress

We now present the results of the yield stress measurements.

The yield stress τ_c was measured with a method which avoids destroying the homogeneity and the isotropy of the suspension. The evolution of the dimensionless yield stress $\tau_c^{\text{hom}}/\tau_c$ as a function of the solid volume fraction φ of noncolloidal particles is depicted in Fig. 5 for the studied materials.

Fig. 5 clearly shows that the yield stress of the suspensions reads as the product of the suspending fluid yield stress times a function $f(\varphi)$. When both the dimensionless yield stresses and the dimensionless elastic moduli are drawn on the same diagram (see Fig. 6), it is obvious that the yield stress function $f(\varphi)$ is different from the elastic modulus function $g(\varphi)$.

It is possible to directly use Eqs. (17), (18) and (19) to evaluate the function $f(\varphi)$.

For the dilute suspensions, the Einstein relation $g^{\text{DL}}(\varphi) = 1 + 5/2\varphi$ is exact to the first order of φ. Introducing this relation in Eqs. (18) and (19) and keeping only the first order terms yield the dilute estimates:

$$\tau_c^{\text{DL}} = \tau_c\,(1 + 3/4\varphi) \tag{24}$$

$$\eta^{\text{DL}} = \eta\left(1 + \frac{7n+3}{4}\varphi\right) \tag{25}$$

The coefficients of growth of these two estimates with the solid volume fraction are different from that of the Einstein law. According to the experimental results depicted in Fig. 6 the change of scale method also predicts that the two functions $g(\varphi)$ and $f(\varphi)$ are different. The only approximation performed to obtain Eqs. (24) and (25) is to assume that a uniform estimate of the secant modulus over the fluid domain enables to accurately estimate the overall properties

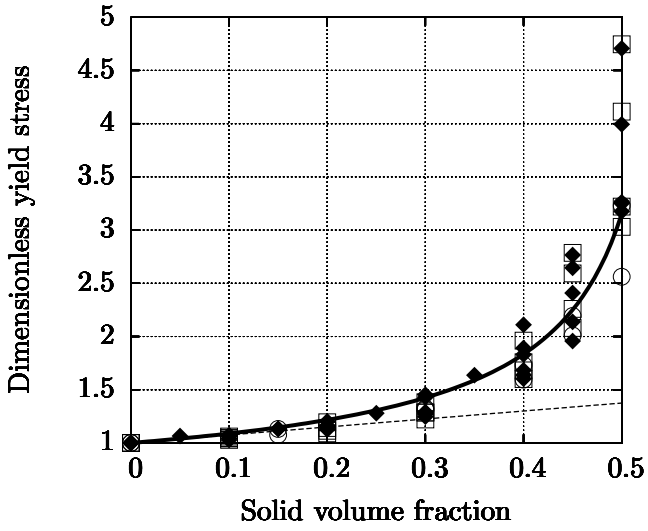

Figure 5: Dimensionless yield stress $\tau_c^{\text{hom}}/\tau_c$ vs the beads volume fraction φ for all the systems studied by Mahaut et al. (2007). The open square symbols are suspensions of polystyrene and glass beads in bentonite, the open circle symbols are suspensions of glass beads in carbopol while the solid diamond symbols are suspensions of polystyrene and glass beads in emulsion. The solid line is the theoretical prediction (26) with $\varphi_m = 0.57$. The dashed curve is the dilute estimate (24) for the yield stress.

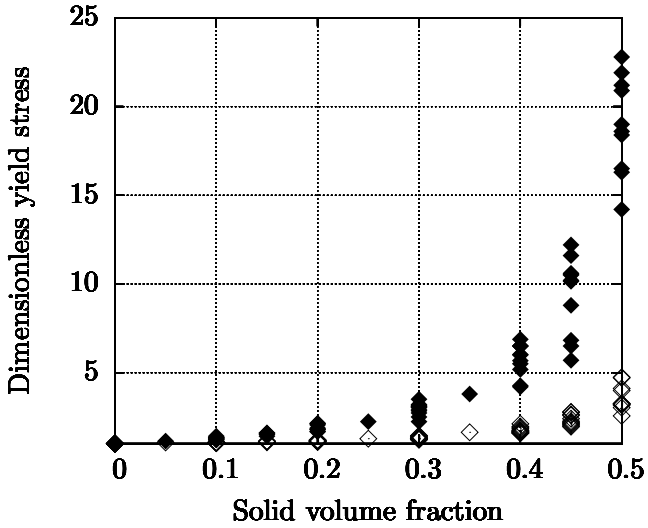

Figure 6: Dimensionless yield stress $\tau_c^{\text{hom}}/\tau_c$ (empty symbols) and dimensionless elastic modulus G^{hom}/G (solid symbols) vs the beads volume fraction φ for all the suspensions studied by Mahaut et al. (2007).

of the suspension. Thus, estimates (24) and (25) are not rigorously exact in contrast with the Einstein law. It is worth noticing that for a suspension of particles in a Bingham fluid, the overall consistency of the suspension is given by the classical Einstein function $1 + 5/2\varphi$.

For larger values of the solid volume fraction, the viscosity of a Newtonian suspension is classically estimated using the Krieger-Dougherty equation [Krieger and Dougherty (1959); Quemada (1985)]. Putting the second equality of Eq. (23) into Eqs. (18) and (19) yields the Krieger-Dougherty estimates for the effective yield stress and the effective consistency of the suspension:

$$\tau_c^{\mathrm{KD}} = \tau_c \sqrt{(1-\varphi)(1-\varphi/\varphi_m)^{-2.5\varphi_m}} \tag{26}$$

$$\eta^{\mathrm{KD}} = \eta\,(1-\varphi)^{\frac{1-n}{2}}\,(1-\varphi/\varphi_m)^{-1.25(n+1)\varphi_m} \tag{27}$$

Both the macroscopic yield stress and the macroscopic consistency diverge when φ tends towards φ_m. The values obtained with Eq. (26) are plotted in Fig. 5, taking $\varphi_m = 0.57$. Good accordance is observed between theoretical and experimental data, accounting for the validity of Eq. (26). Note that no attempt to fit the value of φ_m has been performed.

D Experimental results from the literature

In this paragraph, the theoretical estimates are compared with experimental data of Ancey and Jorrot (2001), Erdogan (2005) and Geiker et al. (2002).

The results for the yield stress are depicted in Fig. 7. The experimental data of Geiker et al. (2002) have not been drawn in Fig. 7 because they report to measure yield stress ten times larger than other researchers.

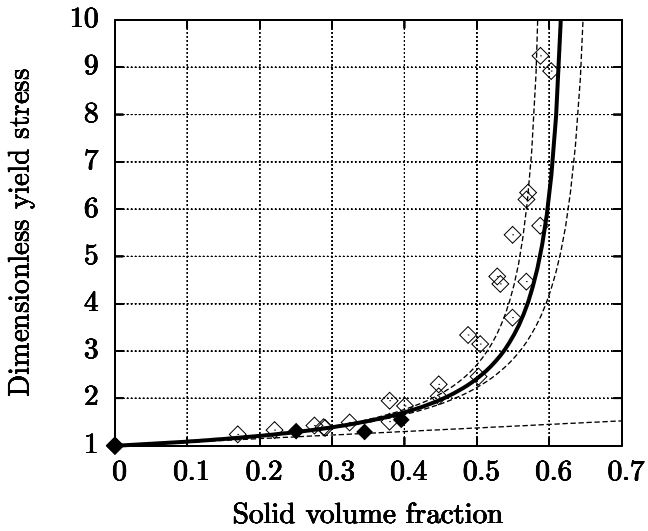

Figure 7: Dimensionless yield stress $\tau_c^{\mathrm{hom}}/\tau_c$ vs beads volume fraction φ for suspensions of Ancey and Jorrot (2001) (empty diamond-shaped) and Erdogan (2005) (solid diamond-shaped). The solid line is the theoretical prediction (26) with $\varphi_m = 0.635$ and the straight dashed line is the dilute overall yield stress (24). The dashed curves are the theoretical Eq. (26) with $\varphi_m = 0.67$ (dashed curve below the solid curve) and $\varphi_m = 0.6$ (dashed curve above the solid curve).

The theoretical curve in Fig. 7 is calculated using $\varphi_m = 0.635$, as reported by Ancey and Jorrot (2001). We also plotted the curve using $\varphi_m = 0.67$ (dashed curve below the solid curve) and $\varphi_m = 0.6$ (dashed curve above the solid curve). The experimental data of Ancey and Jorrot (2001) are roughly well fitted by the theoretical estimate (26) with $\varphi_m = 0.635$ even if the theoretical model always predicts yield stress lower than the measured ones. These discrepancies can not be impart to the experimental procedure. The suspensions was prepared by adding

monodisperse glass beads to a clay dispersion and the yield stress was measured by means of a slump test, an experimental procedure which ensures that the materials remain isotropic and homogeneous. It is believed that the discrepancy between the experimental data of Ancey and Jorrot (2001) and our theoretical predictions could come from a wrong evaluation of the experimental maximum packing fraction. To support this opinion, it is worth noting that the estimate $\varphi_m = 0.635$ of Ancey and Jorrot (2001) was neither measured nor estimated from experimental data. Moreover, this value 0.635 is greater than the values reported in the literature for a dense suspension of non colloidal suspension of monodisperse spherical particles [Ovarlez et al. (2006)]. It can be seen in Fig. 7 that the experimental data are well fitted by Eq. (26) with $\varphi_m = 0.6$.

Erdogan (2005) used a Couette-vane rheometer and applied a strong preshear to the samples before to measure the overall properties of the concrete suspension. Nevertheless, his results compare rather well to the theoretical ones, even if the lack of experimental data for values of the solid fraction larger than 0.4 does not allow to draw a definitve conclusion.

We now pay attention to the results of the consistency measurements. Dimensionless consistency η^{hom}/η measured by Erdogan (2005) and Geiker et al. (2002) are plotted in Fig. 8 as a function of the normalized solid volume fraction φ/φ_m. Four types of aggregates were used by Geiker et al. (2002) : glass beads, sea dredged, crushed, and a mix of 30% sea dredged and 70% crushed aggregates. None of these coarse aggregates are monodisperse (the ratio of the bigger particle size to the smaller one is close to 4 for the all the aggregates). Moreover, only the glass beads are spherical. Then, most of the suspensions studied by Geiker et al. (2002) do not comply with the assumptions made to compute Eqs. (26) and (27).

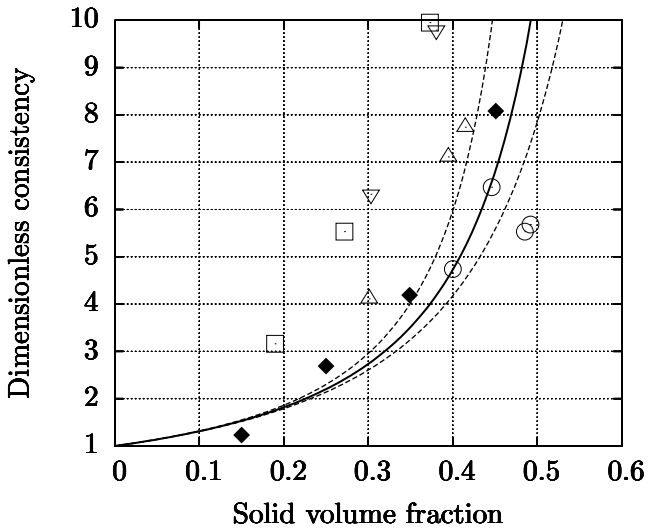

Figure 8: Dimensionless consistency η^{hom}/η vs. the solid volume fraction φ for suspensions of Erdogan (2005) (solid diamond-shaped) and suspensions of Geiker et al. (2002) (empty circle for glass beads, other empty symbols for sea dredged, crushed and mixed aggregates). The solid line is the Krieger-Dougherty estimate for the consistency ($n = 1$) with $\varphi_m = 0.65$. The dashed lines are the same estimate with $\varphi_m = 0.55$ (above the solid curve) and $\varphi_m = 0.75$ (below the solid curve).

Consequently, it is not surprising that the data of Erdogan (2005) are relatively well fitted by the theoretical prediction while the fit between most of the experimental data of Geiker et al. (2002) and the theoretical estimate is less satisfactory. More precisely, while it seems that Eq. (27) is able to roughly estimate the consistency of suspensions of spherical particles (glass beads) even if they are not monodisperse, the discrepancy between experimental and theoretical data is no more acceptable for the other aggregates. As depicted in Fig. 8, tuning the value of

the maximum solid fraction does not allow to improve the quality of the fit.

It is believed that this discrepancy comes from the fact that the sea dredged, crushed and mixed aggregates are not spherical (an aspect ratio equal to 2 has been measured for all these particles). As the Krieger-Dougherty Eq. (23) applies only to suspensions of spherical particles, Eq. (27) cannot fit the properties of suspensions of non-spherical particles. One concludes that using a function $g(\varphi)$ able to accurately estimate the linear properties of a suspension of non spherical particles into Eqs. (18) and (19) will improve the quality of the estimates. This opinion is supported by the fact Geiker et al. (2002) observed that the relative consistency of non-spherical particles suspensions is greater than that of the glass beads suspensions when measured for the same solid volume fraction (see Fig. 8), a trend classically observed for Newtonian suspensions.

V Validity of the theoretical model

For all the results, the experimental data are more dispersed when the solid volume fraction increases and the discrepancy between the experimental and the theoretical results increases when the solid volume fraction tends towards that of the maximum packing fraction. It could be asserted that this discrepancy comes simply from the dispersion of the experimental results. Nevertheless, it is believed that heterogeneities of the secant modulus over the liquid domain are not any more negligible for the larger values of φ. When the solid volume fraction value tends towards the maximum packing fraction, the fluid located near the closest points of two adjacent particles experiences a much larger shear rate than the fluid located far from these points (see Fig. 9). In this situation, it is necessary to take into account the heterogeneities of the secant

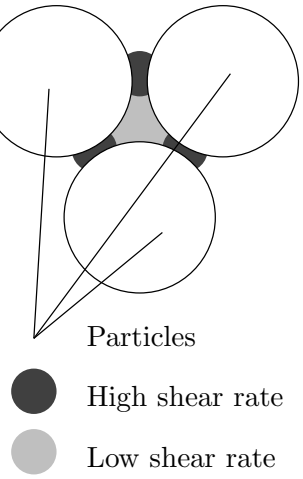

Figure 9: Heterogeneities of the strain rate field for a concentrated suspension.

modulus in the framework of more complex models in order to obtain more accurate estimates.

To use an uniform estimate of the secant modulus induces a second drawback of the model. As no difference is made between all the points located in the fluid phase, such a model is unable to account for the fact that the fluid does not start to flow everywhere at the same time (or more precisely that the yield stress is not reached everywhere at the same time in the fluid domain).

For the Bingham suspension, Castañeda (2003) has shown that beyond the yield stress, the behavior of the suspension is first nonlinear and then asymptotes to a purely linear behavior for higher strain rate values. As this phenomenon is induced by the presence of strong fluctuations of the strain rate field in the fluid phase at the onset of yield which induce fluctuations of the secant modulus, the simplified model described above is not able to account for this nonlinearity.

Nevertheless, it is possible to show that the simplified approach performed in this paper furnishes useful estimates.

Thanks to the properties of the minimization problem (8) it is easily established that the potential $W(\boldsymbol{D})$ admits the following lower bound:

$$W(\boldsymbol{D}) \geq \Phi_1(\boldsymbol{D}) + \Phi_2(\boldsymbol{D}) \tag{28}$$

with

$$\Phi_1(\boldsymbol{D}) = (1-\varphi)\,\tau_c \min_{\boldsymbol{d}\in\mathcal{G}(\boldsymbol{D})} \left\langle \tilde{d} \right\rangle_\ell \tag{29}$$

and

$$\Phi_2(\boldsymbol{D}) = (1-\varphi)\,\frac{\eta}{n+1} \min_{\boldsymbol{d}\in\mathcal{G}(\boldsymbol{D})} \left\langle \tilde{d}^{n+1} \right\rangle_\ell \tag{30}$$

The two quantities Φ_1 and Φ_2 define the effective behavior of two suspensions with the same microstructure as the yield stress suspension.

Φ_1 defines the constitutive law of a suspension of particles embedded in a plastic material obeying the standard flow rule for a von Mises criterion with yield shear stress τ_c. Φ_2 is the overall potential of a suspension of rigid particles dispersed in a fluid whose behavior is described by the incompressible viscous power-law:

$$\boldsymbol{\sigma} = 2\eta\tilde{d}^{n-1}\boldsymbol{d} - p\boldsymbol{\delta} \qquad \mathrm{tr}\boldsymbol{d} = 0 \tag{31}$$

Thanks to the properties of the function $\left\langle \tilde{d}^m \right\rangle_\ell$ for $m \geq 1$ and of the set $\mathcal{G}(\boldsymbol{D})$, it can be shown that the material defined by the potential Φ_1 is an isotropic rigid plastic material and the overall potential Φ_2 is that of an isotropic incompressible viscous material whose overall behavior is described by an homogeneous function of degree n. Moreover, if the suspending fluid obeys the Bingham law ($n = 1$), the effective potential Φ_2 is that of a Newtonian fluid.

Then, we can state that the macroscopic behavior of the isotropic suspension is energetically "underestimated" by a yield stress state law with same exponent as that of the bearing fluid. Both the overall yield criterion and the viscous behavior can be determined through the solution of two homogenization problems allowing to explicitly calculate the lower bound (28). Of course, the overall potential of the yield stress suspension is not the sum of two simple potentials. Nevertheless, it is obvious that the first term of the lower bound (28) prevails for the lower values of the macroscopic strain rate $\boldsymbol{D}$, while for the larger values of the strain rate, the second term must be taken into account. This property allows to show that, although the macroscopic behavior of the suspension is not Herschel-Bulkley, it tends toward that of a yield stress fluid with yield criterion defined by Φ_1 and viscous flow rule described by Φ_2 for respectively the lower values of the macroscopic strain rate (near the yield stress) and the larger values of the macroscopic strain rate (far from the yield stress). These results are summarized in Fig. 10 for a suspension of particles in a Bingham fluid. On the left part of Fig. 10 are drawn the overall potential W and both potentials Φ_1 and Φ_2 as a function of the second invariant of the macroscopic strain rate. For clarity, the lower bound $\Phi_1 + \Phi_2$ is not drawn. The overall behaviors of the suspension and of the materials associated with the potentials Φ_1, Φ_2 and the lower bound $\Phi_1 + \Phi_2$ are depicted on the right part of Fig. 10. This diagram is very similar to the Fig. 3 of Castañeda (2003). $\tilde{\Sigma}$ denotes the second invariant of the macroscopic deviatoric stress tensor.

Interestingly, using the method described in section III, it can be shown that Eqs (26) and (27) allow to estimate the value of the yield stress defined by Φ_1 and the value of the consistency defined by Φ_2. Then, even if the overall behavior of the suspension is not exactly Herschel-Bulkley, the estimates (26) and (27) can account for well defined properties of the suspension. Nevertheless it must be kept in mind that these estimates are not associated to lower bounds of the potentials Φ_1 and Φ_2. A more accurate estimate for the overall behavior of

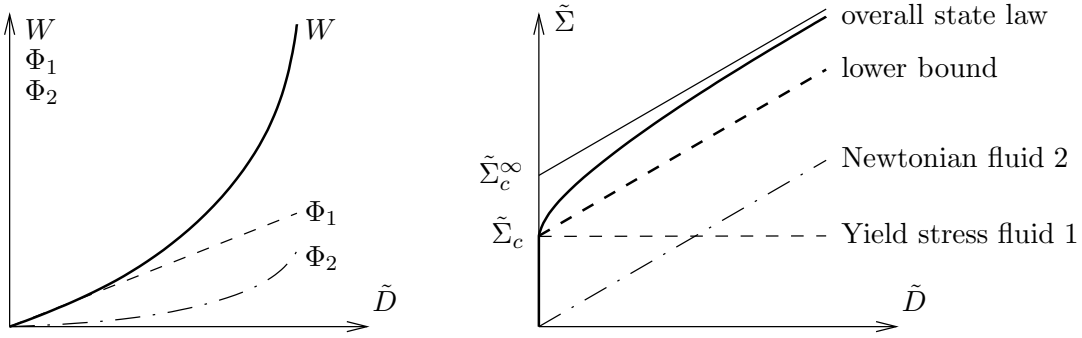

Figure 10: One-dimensional sketch of the functions W, Φ_1 and Φ_2 as a function of the second invariant of $\boldsymbol{D}$ (left). The associated state laws (fictitious materials, lower bound and overall material) are depicted on the right part of the figure. The suspending fluid is Bingham ($n = 1$).

a two-dimensional Bingham suspension, which is of the form suggested by the solid curve in the right part of Fig. 10, has been proposed by Castañeda (2003).

It is clear from Fig. 10 that it is not possible to deduce the value of the macroscopic yield stress $\tilde{\Sigma}_c$ from the measurements of the hight limit strain rate behavior of the overall material. Indeed, if one tries to evaluate the overall yield stress of the suspension from the high-limit strain rate behavior as depicted in Fig 10, the obtained estimate, denoted $\tilde{\Sigma}_c^{\infty}$, is higher than the true yield stress $\tilde{\Sigma}_c$ one must apply to make the suspension flowing. It seems that Geiker et al. (2002) used such a procedure to measure the overall yield stress of the concretes they studied. This result could explain why they measured yield stress values much higher (ten times) than the ones measured by others authors.

The theory predicts that for the higher values of the macroscopic shear rate, the particles do not change the power-law index n. This result is in agreement with previous theoretical and experimental approaches to the rheological properties of concentrated suspensions in non-Newtonian fluid [Polinski et al. (1988); Castañeda (2003)].

VI Conclusion

Theoretical estimates for the overall rheological properties of a suspension of noncolloidal and non-Brownian particles immersed in a nonlinear fluid have been proposed. To our knowledge, this approach and the associated estimates are original in the field of rheology. As the problem to be solved is nonlinear, it was necessary to make some approximations in order to compute simple analytical estimates. Here, the estimates are valid provided that the heterogeneities of the secant modulus can be neglected over the domain filled by the fluid phase. Then, the overall properties of the nonlinear suspension are estimated from that of a fictitious linear suspension having the same microstructure.

In the case where the suspending fluid obeys a Herschel-Bulkley law, the estimates for the yield stress and the consistency read $\tau_c^{\text{hom}}/\tau_c = \sqrt{(1-\varphi)g(\varphi)}$ and $\eta^{\text{hom}}/\eta = \sqrt{g(\varphi)^{n+1}/(1-\varphi)^{n-1}}$ where $g(\varphi)$ denotes the ratio of the macroscopic to the microscopic properties of the fictitious linear material.

Comparison of the theoretical results with experimental data for suspensions of monodisperse rigid noncolloidal particles dispersed in yield stress fluids have also been presented. The experimental procedure used to obtained these data was designed by Mahaut et al. (2007) to evaluate the purely mechanical contribution of the particles to the paste behavior, independently of the physicochemical properties of the materials.

It was found from both the theoretical and the experimental approaches that the dimension-

less yield stress and the dimensionless consistency depend on the bead volume fraction only. It has been shown that the yield stress/solid volume fraction and the consistency/solid volume fraction relationships are well fitted to the very simple laws $\tau_c^{\text{hom}}/\tau_c = (1-\varphi)^{1/2}(1-\varphi/\varphi_m)^{-1.25\varphi_m}$ and $\eta^{\text{hom}}/\eta = (1-\varphi)^{(1-n)/2}\,(1-\varphi/\varphi_m)^{-1.25(n+1)\varphi_m}$ respectively.

As long as the coarse particles are spherical, the theoretical estimates agree quite well with experimental data found in the literature even if experimental procedures used by the authors do not exactly comply with the assumptions made to obtain the theoretical results. This is all the more satisfactory that only four numbers are necessary to calculate the estimates of the overall properties of the suspension as a function of the solid volume fraction: the close packing density of the particles and three suspending fluid properties (yield stress, consistency and power law index).

We now plan to study the case of polydisperse systems and that of anisotropic particle distributions. To improve the theoretical estimates, it will also be necessary to separate the fluid domain in several geometrical domains in order to better describe the heterogeneities over the liquid domain. In particular this situation is expected to be founded for higher values of the solid volume fraction or for polydisperse suspensions.

References

C. Ancey and H. Jorrot. Yield stress for particle suspensions within a clay dispersion. *J. Rheol.*, 45(2):297–319, 2001.

G. K. Batchelor. The stress generated in a non-dilute suspension of particles by pure straining motion. *J. Fluid. Mech.*, 46(4):813–829, 1971.

G. K. Batchelor. The effect of brownian motion on the bulk stress in a suspension of spherical particles. *J. Fluid. Mech.*, 83(1):97–111, 1977.

G. K. Batchelor and J. T. Green. The determination of the bulk stress in a suspension of spherical particles to order c^2. *J. Fluid. Mech.*, 56(3):401–427, 1972.

G. Bossis and J. F. Brady. Dynamic simulation of sheared suspension. i. general method. *J. Chem. Phys.*, 80(10):5141–5154, 1984.

J. F. Brady. Computer simulation of viscous suspensions. *Chem. Eng. Sci.*, 56:2921–2926, 2001.

J. F. Brady and G. Bossis. Stokesian dynamics. *Ann. Rev. Fluid. Mech.*, 20:111–157, 1988.

P. Ponte Castañeda. The effective mechanical properties of nonlinear isotropic composites. *J. Mech. Phys. Solids*, 39(1):45–71, 1991.

P. Ponte Castañeda. Exact second-order estimates for the effective mechanical properties of nonlinear composite materials. *J. Mech. Phys. Solids*, 44(6):827–862, 1996.

P. Ponte Castañeda. On the homogenized behaviour of reinforced and other bingham composites. *Phil. Trans. R. Soc. Lond. A*, 361:947–967, 2003.

A. Einstein. Eine neue bestimmung der molekü ldimensionen. *Ann. Phys.*, 19:289–306, 1906.

T. S. Erdogan. *Determination of aggregate shape properties using X-ray tomographic methods and the effect of shape on concrete rheology.* PhD thesis, University of Texas at Austin, 2005.

R. J. Farris. Prediction of the viscosity of multimodal suspensions from unimodal viscosity data. *Transactions of the society of rheology*, 12(2):281–301, 1968.

N. A. Frankel and A. Acrivos. On the viscosity of a concentrated suspension of solid spheres. *Chem. Eng. Sci.*, 22:847–853, 1967.

M.R. Geiker, M. Brandl, L. N. Thrane, and L. F. Nielsen. On the effect of coarse aggregate fraction and shape on the rheological properties of self-compacting concrete. *Cement, Concrete and Aggregates*, 24(1):3–6, 2002.

R. Hill. Elastic properties of reinforced solids: some theoretical principles. *J. Mech. Phys. Solids*, 11:357–372, 1963.

A. A. Johnson and T. E. Tezduyar. 3d simulation of fluid-particle interactions with the number of particles reaching 100. *Comput. Methods Appl. Mech. Engrg.*, 145(3-4):301–321, 1997.

W. Kreher. Residual stresses and stored elastic energy of composites and polycristals. *J. Mech. Phys. Solids*, 1:115–128, 1990.

I. M. Krieger and T. J. Dougherty. A mechanism for non-newtonian flow in suspensions of rigid spheres. *Transactions of the society of rheology*, III:137–152, 1959.

F. Mahaut, X. Chateau, P. Coussot, and G. Ovarlez. Yield stress and elastic modulus of suspensions of noncolloidal particles in yield stress fluids. *J. of Rheol.*, page Submitted, 2007.

G. Ovarlez, F. Bertrand, and S. Rodts. Local determination of the constitutive law of dense suspension of non colloidal particles through magnetic resonance imaging. *J. Rheol.*, 50(3): 259–292, 2006.

F. Parsi and F. Gadala-Maria. Fore-and-aft asymmetry in a concentrated suspension of solid spheres. *J. Rheol.*, 31(8):725–732, 1987.

A. J. Polinski, M. E. Ryan, R. K. Gupta, S. G. Seshadri, and F. J. Frechette. Rheological behavior of filled polymeric systems i. yield stress and shear-thinning effects. *J. Rheol.*, 32(7): 703–735, 1988.

D. Quemada. Phenomenological rheology of concentrated dispersions - i clustering effects and the structure-dependent packing fraction. *J. Mécan. Théor. Appl.*, SP. Iss:267–288, 1985.

N. Roquet and P. Saramito. An adaptive finite element method for bingham fluid flows around a cylinder. *Computer methods in applied mechanics and engineering*, 192(31-32):3317–3341, 2003.

W. B. Russel, D. A. Saville, and W. R. Schowalter. *Colloidal Dispersions*. Cambridge University Press, Cambridge, 1995.

M. Z. Sengun and R. F. Probstein. Bimodal modal of slurry viscocity with application to coal-slurries. part 1., theory and experiment. *Rheol. Acta*, 28:383–393, 1989a.

M. Z. Sengun and R. F. Probstein. Bimodal modal of slurry viscocity with application to coal-slurries. part 2. high shearlimit behavior. *Rheol. Acta*, 28:394–401, 1989b.

P. Suquet. Overall potentials and extremal surfaces of power-law or ideally plastic materials. *J. Mech. Phys. Solids*, 41:981–1002, 1993.

P. Suquet, editor. *Continuum micromechanics*. Springer-verlag, Wien New York, 1997.

P. Ponte Castañeda & P. Suquet. Nonlinear composites. *Adv. Appl. Mech.*, 34:171–302, 1998.

Z. Yu and A. Wachs. A fictitious domain method for dynamic simulation of particle sedimentation in bingham fluids. *J. Non-Newtonian Fluid Mech.*, doi:10.1016/j.jnnfm.2007.02.007, 2007.

A. Zaoui. Continuum micromechanics: Survey. *ASCE Journal of Engineering Mechanics*, 128 (8):808–816, 2002.